Oil Shale, 2013, Vol. 30, No. 2, pp. 101–116
doi: 10.3176/oil.2013.2.02
ISSN 0208-189X

GEOCHEMICAL INVESTIGATION OF LACUSTRINE OIL SHALE IN THE LUNPOLA BASIN (TIBET): IMPLICATIONS FOR PALEOENVIRONMENT AND PALEOCLIMATE

TAO SUN[(a)(b)], CHENGSHAN WANG[(a)(b)*], YALIN LI[(a)(b)], LICHENG WANG[(c)], JIANGLIN HE[(d)]

[(a)] School of Earth Science and Resources, China University of Geosciences, Beijing 100083, China
[(b)] State Key Laboratory of Geological Process and Mineral Resources, China University of Geosciences, Beijing 100083, China
[(c)] Institute of Mineral Resources, Chinese Academy of Geological Sciences, Beijing 100083, China
[(d)] Chengdu Institute of Geology and Mineral Resources, Chengdu 610000, China

Abstract. *The Dingqinghu Formation oil shale, located in the centre of the Lunpola basin, represents a potential large lacustrine oil shale resource in Tibet. A geochemical investigation of the oil shale was performed to reconstruct paleoenvironment and paleoclimate during deposition. The total organic carbon (TOC) contents (1.46–11.85%), S_2 values (4.79–115.80 mg HC/mg rock) and HI (328–1040 mg HC/mg TOC) of oil shale samples are high, and indicate that the oil shale has a good oil source rock potential. The thermal maturity assessed from PI (0.01–0.09) and T_{max} (429–440 °C) shows an immature to early mature stage of the organic matter. The oil shale exhibits characteristics of odd-over-even predominance, maximum n-alkanes peak at nC_{25} or nC_{23}, a higher proportion of C_{29} sterane, low $\delta^{13}C_{org}$ values (–29.9 to –26.7‰), a low Pr/Ph ratio (0.03–0.40), high values of the gammacerane index (up to 25.24), and presence of β-carotane, which is consistent with a reducing, stratified and hypersaline palaeo-lake with the main contribution of algae and bacteria to the organic matter (OM). The development history of palaeo-lakes from the Oligocene to the Early Miocene indicates that the climate of the Lunpola basin region during the deposition of oil shale was arid.*

Keywords: *geochemistry, paleoenvironment, paleoclimate, oil shale, Lunpola basin.*

* Corresponding author: e-mail *chshwang@cugb.edu.cn*

1. Introduction

Oil shale deposits are widespread in China, and proved reserves amount to about 32 billion tons, representing a potential energy source [1]. Tertiary oil shales, such as Fushun and Maoming ones, were mainly formed in lacustrine environments [1–3].

Research about oil shale in Tibet has made some breakthrough in recent years and some articles about marine oil shale have been published [4–7]. However, lacustrine oil shale in the Lunpola basin has received less attention, although oil shale in this basin was first mentioned by Xu already in 1984 [8].

In this paper, geochemical investigations of the Lunpola basin lacustrine oil shale are described systematically. The primary aim is to interpret the paleoenvironment and paleoclimate during oil shale deposition. The results also provide geologists worldwide information about the geochemistry of oil shale in the Tertiary continental sedimentary basin in Tibet.

2. Geological setting

The Lunpola basin is a primarily Tertiary sedimentary basin situated in the central part of the Tibetan plateau (Fig. 1). The basin axis strikes mainly east-west and has been variably deformed along basin-parallel thrust faults and associated folds. Erosion through these structures has exposed much of the succession at the surface. The Lunpola basin contains a thick stratigraphic succession that extends from the Palaeocene to the Pliocene [9]. The basin has been explored geophysically and through a series of wells that has established the stratigraphic context and correlation of sediments within the basin [10].

The basin base consists of Mesozoic strata, which are composed of marine carbonate, clastic rocks, mafic lava and volcaniclastic units [11–12]. The Cenozoic strata of the Lunpola basin are more than 4000 m thick, and consist of two primary stratigraphic units: the Niubao Formation and the overlying Dingqinghu Formation. The age of these formations was determined to be the Paleocene-Oligocene and Miocene-Pliocene, respectively [13–15], based primarily on fossil ostracod and palynological assemblages. More recent investigation indicated that the Niubao and Dingqinghu formations are Paleocene-Eocene and Oligocene, respectively [16–17]. The Dingqinghu Formation discussed herein mainly consists of dark mudstone, marlstone, oil shale, siltstone and shale, and contains ostracods and green algae identified in exploration wells [12].

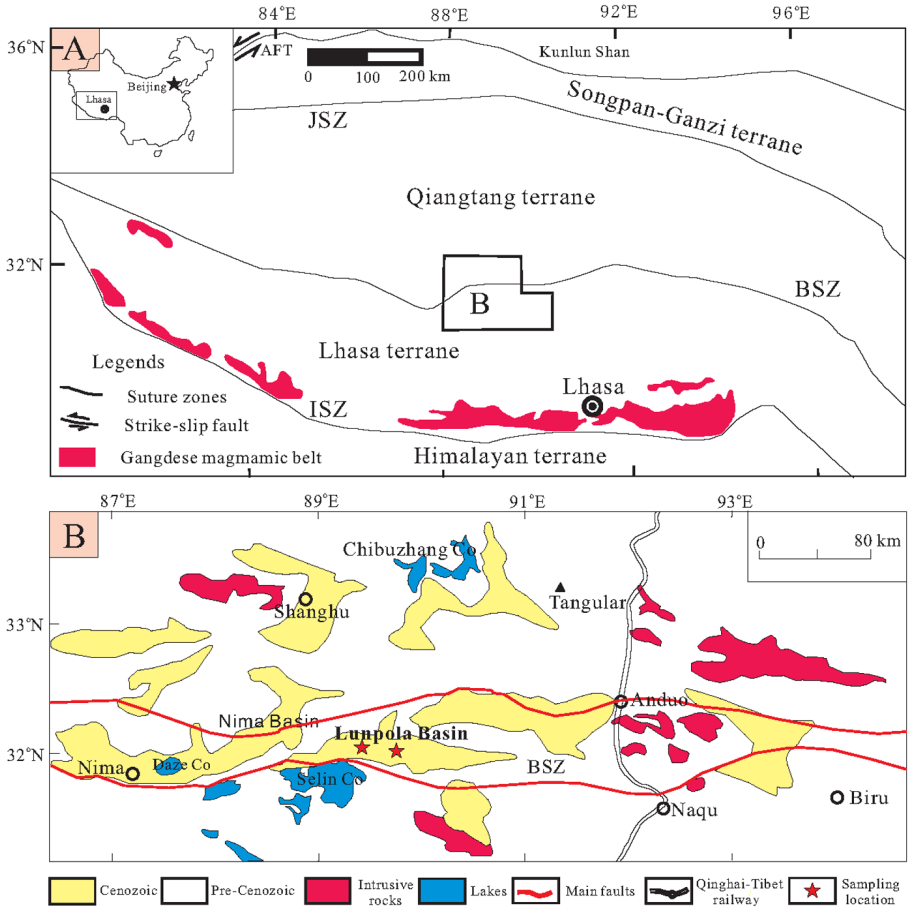

Fig. 1. (A) Tectonic map of the Tibetan plateau, after DeCelles et al. [17]. (B) Simplified geological map of the central Tibet showing the location of Lunpola basin oil shale. ATF: Altyn Tagh fault; BSZ: Banggong suture zone; JSZ: Jingsha suture zone; ISZ: Indus-Yarlung suture zone.

3. Samples and tests

The study profiles (LP01 and LP02) are located in the central part of the Lunpola basin (Fig. 1B). A total of 26 samples were collected from the two profiles. All samples were collected for geochemical analyses. Details of sampling locations and rock assemblages are shown in Figure 2.

Total organic matter (TOC) was determined on a LECO CS-200 apparatus (BGR, Germany). About 100 mg of sample (ground to 120 mesh) was heated from ambient temperature up to 1200 °C in an induction furnace after removing carbonate with hydrochloric acid (HCl). Standard deviations are less than 0.5%. Pyrolysis data were collected using a Rock-Eval II

apparatus (Petrobas Research Centre, France). A 100 mg crushed sample (120 mesh) was analyzed following guidelines established by Peters [18].

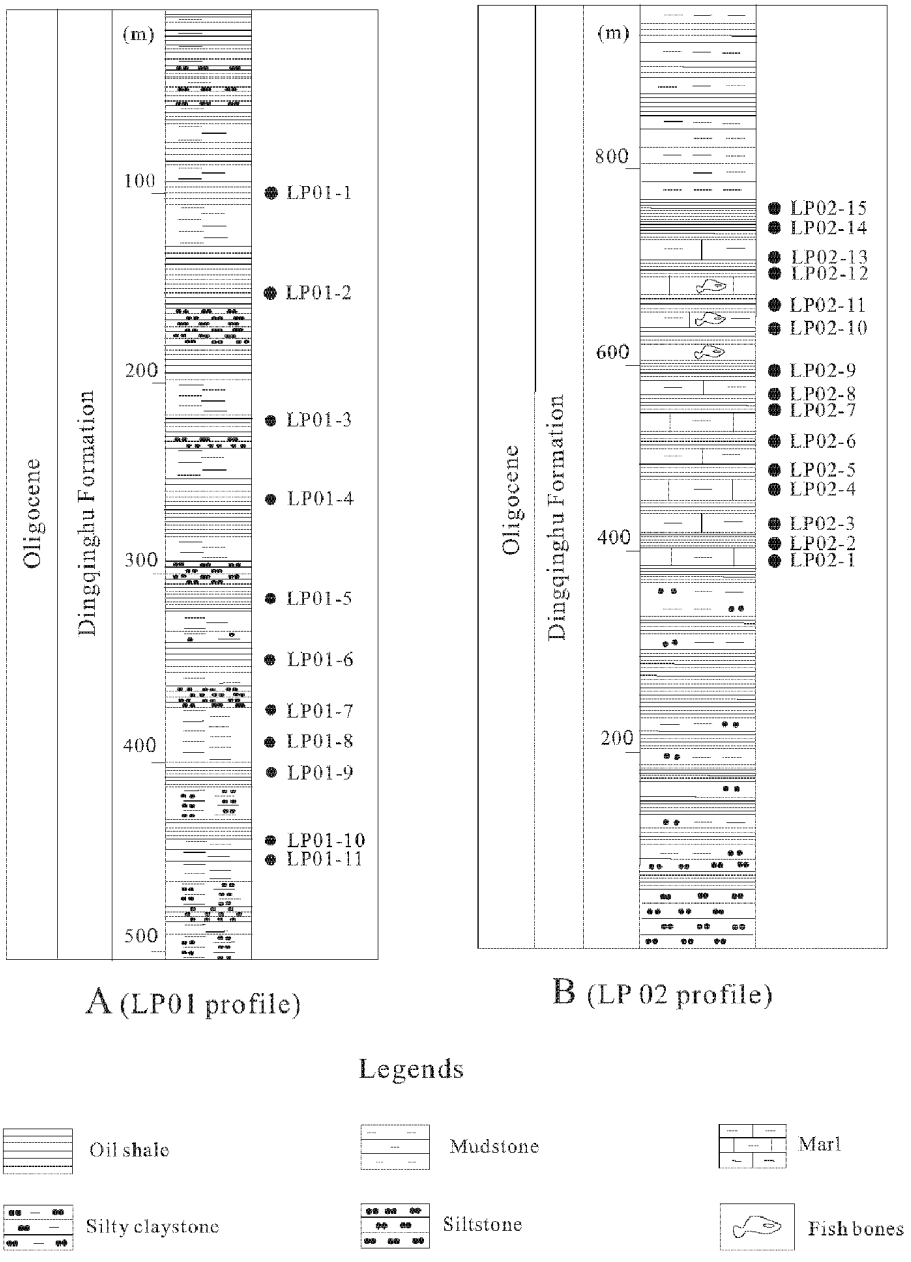

Fig. 2. Stratigraphic columns for LP01 (A) and LP02 (B) profiles in the Lunpola basin. Sample depths are indicated on the columns.

The powdered samples to be analyzed were extracted with chloroform for 72 h in a Soxhlet apparatus. The extractable organic matter was separated by column chromatography into saturated hydrocarbons, aromatic hydrocarbons and NSO compounds by using a silica gel alumina column, after precipitation of asphaltenes [19]. Gas chromatography (GC) was carried out with an Agilent 6890 N gas chromatograph (Agilent Technologies, Inc., USA) equipped with a 30 m × 0.20 mm ID × 0.2 μm film silica column. The oven temperature was programmed from 70 to 300 °C at a rate of 8 °C/min and held at 300 °C for 20 min. Injection was performed in the split/splitless mode with a splitless time of 60 s. Helium was used as a carrier gas (injection temperature 310 °C). GC/MS analysis was carried out using a TRACE2000/SSQ-7000 mass spectrometer (Triplemass, Netherlands). A 30 m × 0.20 mm ID × 0.2 μm film Varina CP Sil-8CB fused silica column was used. Helium was used as carrier gas. The temperature was programmed from 80 to 160 °C at a rate of 8 °C/min and from 160 to 310 °C at a rate of 2.8 °C/min, with a 5 min isothermal period at 310 °C.

To prepare kerogens, fragments of rock were leached in 12 N HCl for 12 h to remove carbonates, then washed several times with distilled water and treated with hydrofluoric acid (HF) for 12 h to remove silicates [20]. The samples were again washed several times with distilled water and again treated with 12 N HCl [20]. A visual estimation of the relative abundance of maceral content was made using a Zeiss incident-light microscope and a Swift point counter (Canimpex Enterprises Ltd., Canada) [19]. Elemental analyses were performed on a FLASH EA-1112 Series elemental analyzer (Conquer Scientific, USA) with a precision generally around 0.3% for carbon and 0.5% for nitrogen. The $\delta^{13}C$ kerogen isotopic measurements were determined on an EA-Finnigan Delta plus XL mass spectrometer. The results of carbon isotope analysis are reported in the usual δ-notation relative to the PDB standard; the analytical precision by this method was better than ±0.2‰ [5]. All analyses were performed in the Organic Geochemistry Laboratory, Research Institute of Exploration and Development, Huabei Oilfield Branch Company of PetroChina.

4. Results and discussion

4.1. TOC and Rock-Eval

Rock-Eval and TOC data are summarized in Table 1. The TOC contents of six oil shale samples from the LP01 profile vary from 2.84 to 6.92%, whereas mudstone samples contain 0.25 to 5.99% TOC (Table 1). The S_2 values of oil shale samples are in the range of 12.75–57.38 mg HC/g rock, compared to 0.90–50.45 mg HC/g rock for mudstone samples (Table 1). The HI of oil shale samples from the LP01 profile varies between 449 and 841 mg HC/g TOC. The high S_2 and HI values clearly indicate that the oil shale from the LP01 profile has a good source-rock potential. All analyzed samples from the LP01 profile are characterized by relatively low PI

(0.01–0.46) and T_{max} values (427–438) (Table 1) indicating that the organic matter is thermally immature to early mature.

The twelve oil shale samples from the LP02 profile have TOC contents varying between 1.46 and 11.85%, whereas three marlstone samples contain 0.28 to 1.04% TOC (Table 1). The high S_2 values of 4.79–115.80 mg HC/mg rock and HI values of 328–1040 HC/g TOC (Table 1) indicate that oil shale from the LP02 profile has a good source-rock potential, whereas the

Table 1. Results of Rock-Eval and TOC analysis and calculated parameters

Sample No.	Lithology	TOC[a], wt%	S_1[b], mg HC[c]/g	S_2[d], mg HC/g	PY[e] (S_1+S_2), mg HC/g	T_{max}[f], °C	HI[g], HC/g TOC	PI[h] (S_1/(S_1+S_2))
LP01-1	Shale	2.84	0.51	12.75	13.26	438	449	0.04
LP01-2	Shale	6.56	1.17	51.99	53.16	433	793	0.02
LP01-3	Shale	6.92	0.83	57.38	58.21	434	829	0.01
LP01-4	Shale	3.89	0.59	30.55	31.14	436	785	0.02
LP01-5	Shale	5.12	1.09	39.84	40.93	432	778	0.03
LP01-6	Shale	4.82	0.80	40.54	41.34	429	841	0.02
LP01-7	Mudstone	3.29	0.99	29.86	30.85	438	908	0.03
LP01-8	Mudstone	5.95	2.52	50.45	52.97	433	848	0.05
LP01-9	Mudstone	0.25	0.76	0.90	1.66	431	360	0.46
LP01-10	Mudstone	5.99	2.62	54.16	56.78	432	904	0.05
LP01-11	Mudstone	0.87	1.02	6.21	7.23	427	714	0.14
LP02-1	Marl	1.04	0.08	1.75	1.83	433	168	0.04
LP02-2	Shale	1.46	0.04	4.79	4.83	442	328	0.01
LP02-3	Marl	0.31	0.03	0.40	0.43	419	129	0.07
LP02-4	Marl	0.28	0.02	0.32	0.34	423	114	0.06
LP02-5	Shale	4.75	0.13	34.47	34.6	436	726	0.00
LP02-6	Shale	2.39	0.34	14.70	15.04	431	615	0.02
LP02-7	Shale	4.29	0.42	33.06	33.48	435	771	0.01
LP02-8	Shale	6.25	5.12	49.77	54.89	413	796	0.09
LP02-9	Shale	10.15	1.06	105.51	106.57	440	1040	0.01
LP02-10	Shale	7.65	0.69	66.02	66.71	432	863	0.01
LP02-11	Shale	11.85	2.34	115.80	118.14	436	977	0.02
LP02-12	Shale	7.95	0.73	78.33	79.06	438	985	0.01
LP02-13	Shale	13.05	4.97	96.95	101.92	439	743	0.05
LP02-14	Shale	6.24	0.54	53.97	54.51	435	865	0.01
LP02-15	Shale	11.95	3.59	97.80	101.39	440	818	0.04

[a] TOC = total organic carbon.
[b] S_1 = free hydrocarbons.
[c] HC = hydrocarbon.
[d] S_2 = pyrolysable hydrocarbons.
[e] PY = potential yield.
[f] T_{max} = temperature of maximum S_2.
[g] HI = hydrogen index.
[h] PI = production index.

source-rock potential of marlstone is relatively low. T_{max} values for all the samples mostly fall within the range of 430–440 °C indicating that the samples are thermally immature to early mature.

4.2. Element and stable carbon isotopic composition of kerogen

The elemental analysis data are listed in Table 2. The H/C ratio of oil shale from the LP01 profile varies between 1.44 and 1.63 and that of O/C between 0.13 and 0.14 (Table 2). The H/C and O/C ratios of twelve oil shale samples from the LP02 profile range from 1.36 to 1.63 and 0.12 to 0.14, respectively. Based on these ratios (Fig. 3), the organic matter in oil shale samples from LP01 and LP02 profiles can be classified as Type I kerogen (except for samples LP02-2 and LP02-6) (Fig. 3) and marlstone as Type II. Type I kerogen mainly originated from planktonic green algae or amorphous organic matter [21]. The high HI values (> 700 mg HC/g TOC) in most oil shale samples support the algal or bacterial contribution to the organic matter [22].

The oil shale from LP01 and LP02 profiles have a similar heavy C isotopic composition, ranging in $\delta^{13}C$ values of the bulk organic matter from

Table 2. Results of analysis of organic elements and carbon isotopes of samples from LP01 and LP02 profiles in the Lunpola basin

Sample No.	Lithology	C, wt%	H, wt%	O, wt%	H/C ratio	O/C ratio	$\delta^{13}C_{PDB}$/‰
LP01-1	Shale	68.94	8.59	12.56	1.49	0.14	–26.7
LP01-2	Shale	66.74	8.21	12.76	1.48	0.14	–29.6
LP01-3	Shale	68.26	9.26	11.36	1.63	0.12	–28.5
LP01-4	Shale	66.51	8.85	11.25	1.60	0.13	–28.6
LP01-5	Shale	67.56	8.74	11.89	1.55	0.13	–28.8
LP01-6	Shale	68.58	8.22	11.60	1.44	0.13	–27.2
LP01-7	Mudstone	68.11	8.01	11.39	1.41	0.13	–27.6
LP01-8	Mudstone	69.45	8.42	10.73	1.46	0.12	–27.9
LP01-9	Mudstone	69.66	8.43	11.31	1.45	0.12	–25.7
LP01-11	Mudstone	60.50	6.94	9.87	1.38	0.12	–28.2
LP02-1	Marl	75.20	8.46	15.04	1.35	0.15	–27.9
LP02-2	Shale	72.09	8.23	12.50	1.37	0.13	–29.7
LP02-3	Marl	81.51	8.83	16.30	1.30	0.15	–27.8
LP02-4	Marl	87.20	8.72	17.44	1.20	0.15	–26.3
LP02-5	Shale	68.38	9.06	10.94	1.59	0.12	–29.9
LP02-6	Shale	74.65	8.46	13.93	1.36	0.14	–28.8
LP02-7	Shale	69.76	8.72	10.23	1.50	0.11	–27.5
LP02-8	Shale	69.87	8.85	11.18	1.52	0.12	–27.3
LP02-9	Shale	67.14	9.12	10.74	1.63	0.12	–28.5
LP02-10	Shale	67.28	8.69	11.66	1.55	0.13	–29.7
LP02-11	Shale	67.00	8.71	10.72	1.56	0.12	–28.3
LP02-12	Shale	65.81	8.61	10.53	1.57	0.12	–27.9
LP02-13	Shale	64.05	8.38	10.25	1.57	0.12	–27.9
LP02-14	Shale	68.18	9.09	10.91	1.60	0.12	–29.1
LP02-15	Shale	66.15	8.82	10.58	1.60	0.12	–28.9

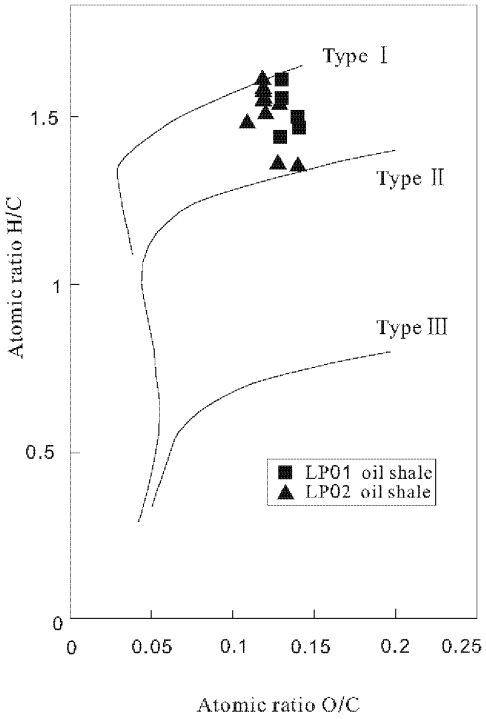

Fig. 3. Plot of H/C versus O/C of kerogen from oil shale samples from LP01 and LP02 profiles showing organic matter type.

–29.6 to –26.7‰ and –29.9 to –27.3‰, respectively (Table 2). The oil shale shows no enrichment in ^{13}C, which is different from the Tertiary lacustrine Duatinga oil shale in Australia [23]. Regional organic facies variations caused by bioassemblage input or significant climatic fluctuation [22], or water column productivity variation [5, 24] may result in differences in stable carbon isotope compositions. Enrichment in ^{13}C seems to be a common feature in hypersaline systems. Hypersalinity itself has been suggested to be the cause for these heavy isotope values in microbial mats [25]. As discussed below, the Lunpola basin oil shale, mudstone and marlstone were deposited in hypersaline environments, and the organic matter derived from these rocks should exhibit similar enrichment and consistent isotopic trends. Therefore, organic facies variations may be the main reason for lower $\delta^{13}C_{org}$ values (–29.9 to –26.7‰) of oil shale. Lewan [26] proposed that the phytoplankton residing in environments that are dominated by organic-derived CO_2 results in amorphous kerogens, which are expected to occur in restricted basins that are overlain by stratified shallow (<200 m) water. The Lunpola palaeo-lake was a stratified and shallow water lake. Therefore, it is suggested that lacustrine algae are considered to be the precursors of amorphous kerogens and the isotopically low carbon isotopic values are attributed to lacustrine algae.

4.3. Molecular composition of organic matter

4.3.1. *n*- and *iso*-alkanes

Gas chromatograms of the saturated hydrocarbons isolated from LP01 and LP02 oil shale samples are presented in Figure 4 and their parameters are given in Table 3. The analyzed samples contain abundant C_{15+} *n*-alkanes indicating a slight biodegradation at the most [27] (Fig. 4). The *n*-alkanes patterns of oil shale from both profiles are dominated by long-chain n-alkanes with a marked odd-over-even preference in the nC_{23} to nC_{31} range (most samples having the carbon preference index CPI > 3) with the exception of the sample LP01-6. Long-chain *n*-alkanes (n-C_{27} to n-C_{31}) are known as biomarkers for higher terrestrial plants waxes [28–29]. The dominance of long-chain *n*-alkanes for the samples LP01-1, LP02-3, LP02-12 and LP02-13 therefore reflects the contribution of terrestrial plants.

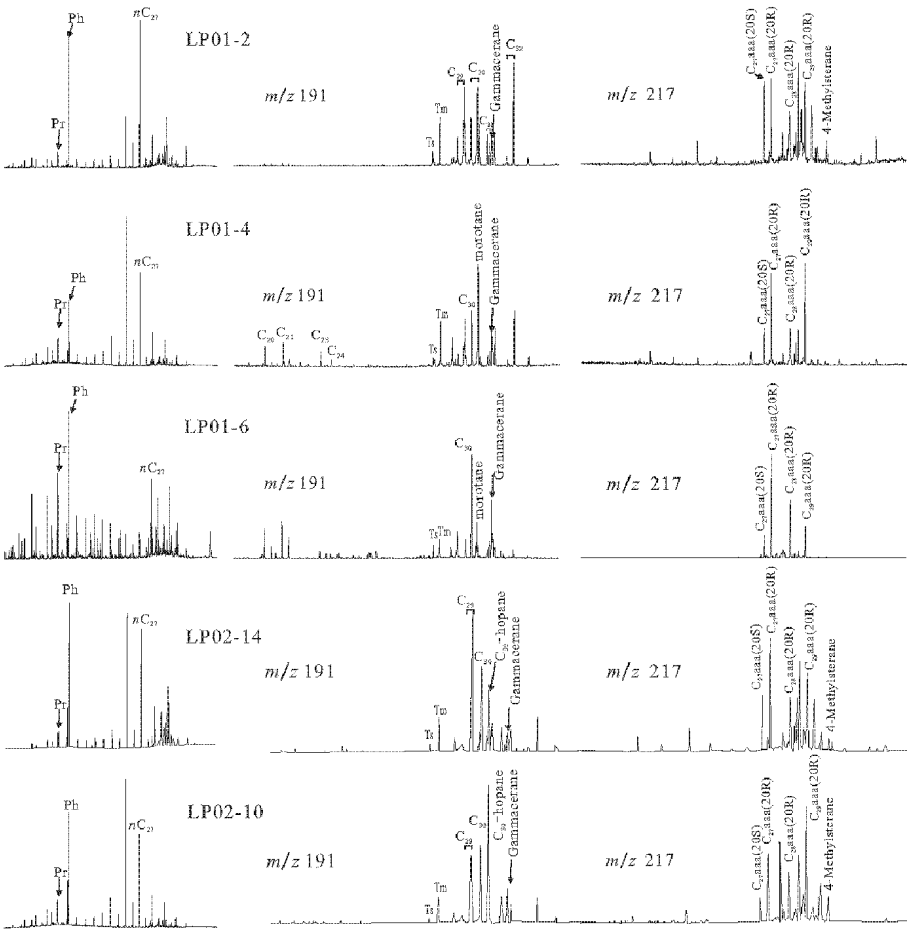

Fig. 4. Gas chromatograms, terpane and sterane mass chromatograms of samples from LP01 and LP02 profiles in the Lunpola basin.

Table 3. Organic geochemical data for extracts of samples from LP01 and LP02 profiles in the Lunpola basin

Sample No.	Pr/nC_{17}	Ph/nC_{18}	Pr/Ph[a]	CPI	$\%C_{27}$[b]	$\%C_{28}$[c]	$\%C_{29}$[d]	Gammacerane index[e]	β-carotane
LP01-1	1.25	10.38	0.18	2.36	29	15	56	2.19	n.d.
LP01-2	0.88	19.15	0.10	4.01	40	23	37	1.04	n.d.
LP01-3	0.95	5.98	0.28	5.42	41	17	42	0.71	present
LP01-4	1.27	4.98	0.40	8.24	40	16	44	2.62	n.d.
LP01-5	1.74	17.08	0.15	4.31	12	12	76	3.96	n.d.
LP01-6	1.01	4.59	0.43	2.19	54	30	16	4.63	n.d.
LP01-7	1.39	5.83	0.35	1.83	57	25	18	5.09	present
LP01-8	1.11	6.37	0.34	2.29	51	28	21	5.55	n.d.
LP01-9	1.18	7.90	0.26	1.84	51	25	24	7.01	n.d.
LP01-10	0.92	2.44	0.42	1.95	47	19	34	2.94	n.d.
LP01-11	2.30	9.77	0.30	1.48	53	19	28	9.93	n.d.
LP02-1	0.83	26.94	0.07	3.54	34	15	51	11.71	n.d.
LP02-2	0.91	12.31	0.14	4.79	40	16	44	8.39	n.d.
LP02-3	1.56	15.54	0.12	2.82	26	12	62	8.11	present
LP02-4	1.27	7.52	0.19	3.76	28	14	58	5.73	present
LP02-5	1.08	59.91	0.05	3.94	35	14	51	25.24	present
LP02-6	1.26	33.45	0.06	4.61	51	21	28	17.37	n.d.
LP02-7	1.41	52.94	0.05	4.64	39	16	45	15.34	n.d.
LP02-8	1.52	85.17	0.03	8.59	40	20	40	3.06	n.d.
LP02-9	1.11	42.80	0.06	2.59	44	17	39	11.26	n.d.
LP02-10	1.27	90.20	0.04	5.10	31	20	49	10.51	n.d.
LP02-11	0.92	58.20	0.04	7.31	30	20	51	5.03	n.d.
LP02-12	1.39	37.00	0.06	3.10	14	19	67	13.85	n.d.
LP02-13	2.18	59.72	0.06	3.79	11	14	75	1.99	n.d.
LP02-14	1.20	15.61	0.13	4.72	48	21	31	3.89	n.d.
LP02-15	1.09	19.80	0.08	5.03	42	17	41	1.34	n.d.

n.d. not detected
[a] Pr/Ph = pristine/phytane ratio.
[b] $\%C_{27} = \%C_{27}\alpha\alpha\alpha R/C_{27}–C_{29}\alpha\alpha\alpha R$-steranes.
[c] $\%C_{28} = \%C_{28}\alpha\alpha\alpha R/C_{27}–C_{29}\alpha\alpha\alpha R$-steranes.
[d] $\%C_{29} = \%C_{27}\alpha\alpha\alpha R/C_{27}–C_{29}\alpha\alpha\alpha R$-steranes.
[e] Gammacerane index = Gammacerane/(C_{31}(22S+22R)/2)

The oil shale samples from LP01 and LP02 profiles exhibit low values of the pristane/phytane (Pr/Ph) ratio ranging from 0.03 to 0.43 (Table 3). The Pr/Ph ratio has been used in many studies to infer the oxic/anoxic character of depositional environments and sources of organic matter. High Pr/Ph ratios are usually associated with organic matter that has undergone oxidation to the extent that the phytol side chain of chlorophyll or related structures has been oxidized, a pathway that leads preferentially to the formation of pristane [30]. However, several factors, such as thermal maturity [31] and variable source input [32], must be taken into account when Pr/Ph ratios are considered. Ten Haven et al. [33] proposed that it is

virtually impossible to draw valid conclusions from Pr/Ph ratio with respect to the redox conditions of the environment of deposition. However, Peters et al. [32] still recommended that Pr/Ph <0.6 indicates anoxic, commonly hypersaline or carbonate environments, whereas Pr/Ph >3.0 typifies terrigenous organic matter input under oxic conditions for rocks within the oil generative window. Maturity variations within the studied samples can be excluded. The low Pr/Ph ratio indicates that these rocks were deposited in anoxic and probably hypersaline conditions, which is supported by the abundant pyrite crystals found in the Lunpola oil shale [34]. Syngenetic pyrite in coal and oil shale indicates an anoxic sedimentary environment [6, 35].

Peters et al. [32] suggested that β-carotane is the most prominent compound of the carotenoid carbon skeleton preserved in sediments under highly reducing conditions. The presence of β-carotane is associated primarily with anoxic, saline lacustrine, or highly restricted marine settings [32, 36]. β-carotane occurs in several oil shale samples from the Lunpola basin (Table 3), indicating an anoxic and saline lacustrine environment. This compound is also reported in Chinese Junggar Permian [37] and Jianghan oil shales [38].

4.3.2. Hopanes and steranes

The gammacerane index varies from 0.71 to 9.93 and 1.34 to 25.24 (Table 3) for LP01 and LP02 profile oil shale, respectively. Gammacerane is a biomarker of highly reducing, hypersaline conditions during deposition of the contributing organic matter [39–40]. Sinninghe Damsté et al. [41] argued that gammacerane indicates a stratified water column in marine and non-marine source rock depositional environments, commonly resulting from hypersalinity at depth. Clearly, because the water columns in hypersaline depositional environments are often density stratified, it may be the reason that the compound is abundant in saline lacustrine deposits [41]. The Lunpola basin oil shale was therefore probably deposited in a highly saline lacustrine environment, which is also supported by the very low Pr/Ph values and the presence of β-carotane. The discovery of gypsum of the Dingqinghu Formation in the Nima basin (west of the Lunpola basin) [17] also supports this interpretation. It is possible that the salinity in the water column remained the same and water-column stratification is constant during most of the time when the Lunpola oil shale deposited, which is supported by the high TOC and HI values of Lunpola basin oil shale samples [21].

Oil shale samples from the LP01 profile show slightly higher C_{29} (37–76%) normal sterane contents compared to those of C_{27} (12–41%) and C_{28} (12–23%) normal steranes (Table 3). A similar distribution of steranes was also observed in the LP02 profile (Table 3), reflecting a contribution of higher terrestrial plants [42]. In contrast, mudstones (e.g., LP01-7) exhibit a different distribution; their C_{29} steranes exhibit a relatively low abundance ranging from 16 to 34%. Huang and Meinschein [43] proposed that the

predominance of C_{29} sterols (steranes) should indicate a strong contribution from the organic matter of higher plants, whereas the prevalence of C_{27} sterols (steranes) should imply the dominance of marine plankton. Based on this interpretation, the relative amount of steranes was used to infer biological sources of organic matter in oils [44]. However, we should be careful when interpreting C_{29} sterane predominances. Volkman [45] found that marine sediments, including those deposited in pelagic environments far from terrigenous influence, showed the predominance of C_{29} steranes, and concluded that there must be unproven marine sources of C_{29} steranes. In addition, as illustrated in Figure 4, steranes of the LP01-4 oil shale exhibit a V-shaped pattern, namely $C_{27}>C_{28}<C_{29}$, revealing mixed contributions from algae or bacterial and higher plant wax sources [42].

5. Paleoenvironmental and paleoclimatic significances

It is well known that distribution of lakes, lake productivity and preservation of organic matter are controlled by climatic and tectonic factors. Palaeoclimate and palaeogeography not only play major roles in controlling distribution of lake bodies but also influence water chemistry. It is clear that saline lakes develop when evaporation exceeds precipitation and fresh-water lakes develop when precipitation exceeds evaporation. As discussed above, the Lunpola basin oil shale was deposited in a highly saline lacustrine environment, which indicates arid climate. Other evidence supports this interpretation. Regional uplift in central Tibet at about 40 Ma contributed to an abrupt global cooling and dramatic aridification [46–49]. Climate in the Tibetan plateau became dry after the Eocene/Oligocene transition. DeCelles et al. [17] suggested that considerable lake evaporation and low soil respiration rates existed in the Oligocene of the Nima basin based on the oxygen isotope values in palaeo-lacustrine carbonates and carbon isotope values in palaeosol carbonates, which is indicative of an arid climate. All data probably support a conclusion that the saline palaeo-lakes were widely developed in the central Tibetan plateau in the Oligocene and the climate was arid. Therefore, the climate of the Lunpola basin region during the deposition of oil shale was arid.

6. Conclusions

Twenty-six samples of lacustrine oil shale, mudstone and marlstone from LP01 and LP02 profiles in the Lunpola basin have been studied with regard to their organic geochemical characteristics. The TOC contents and S_2 values of oil shale samples from LP01 and LP02 profiles in the Lunpola basin are high, indicating that this oil shale has a good source-rock potential. The thermal maturity assessed from PI and T_{max} shows an immature to early

mature stage of the organic matter. The Lunpola basin oil shale exhibits characteristics of odd-over-even predominance, maximum *n*-alkanes peak at nC_{25} or nC_{23}, a higher proportion of C_{29} sterane, low $\delta^{13}C_{org}$ values, a low Pr/Ph ratio, high values of the gammacerane index, and presence of β-carotane, which is consistent with a reducing, stratified and hypersaline palaeo-lake with the main contribution of algae and bacteria to the organic matter. A highly saline lacustrine environment and regional uplift in central Tibet at about 40 Ma suggest that the climate of the Lunpola basin region during the deposition of oil shale was probably cool and arid.

Acknowledgements

The research project was financially supported by the Fundamental Research Funds for the Central Universities (No. 2011PY0238), the National Natural Science Foundation of China (No. 40672086), and the National Petroleum Resources Special Project: Strategic Investigation and Geological Survey on Oil and Gas Resources in Tibet Plateau (No. 1212011221103). The authors are grateful to Dr. Shunping Ma for analytical work.

REFERENCES

1. Qian, J., Wang, S. L. Oil shale development in China. *Oil Shale*, 2003, **20**(3S), 356–359.
2. Brassell, S. C., Eglinton, G., Fu, J. M. Biological marker compounds as indicators of the depositional history of the Maoming oil shale. *Org. Geochem*., 1986, **10**(4–6), 927–941.
3. Zhang, S. C., Zhang, B. M., Bian, L. Z., Jin, Z. J., Wang, D. R., Chen, J. F. The Xiamaling oil shale generated through Rhodophyta over 800 Ma ago. *Sci. China Ser. D-Earth Sci.*, 2007, **50**(4), 527–535.
4. Fu, X. G., Wang, J., Tan, F. W., Zeng, Y. H. Sedimentological investigations of the Shengli River-Changshe Mountain oil shale (China): relationships with oil shale formation. *Oil Shale*, 2009, **26**(3), 373–381.
5. Fu, X. G., Wang, J., Zeng, Y. H., Li, Z. X., Wang, Z. J. Geochemical and palynological investigation of the Shengli River marine oil shale (China): implications for palaeoenvironment and palaeoclimate. *Int. J. Coal Geol.*, 2009, **78**(3), 217–224.
6. Fu, X. G., Wang, J., Zeng, Y. H., Tan, F. W., Feng, X. L. REE geochemistry of marine oil shale from the Changshe Mountain area, northern Tibet, China. *Int. J. Coal Geol*., 2010, **81**(3), 191–199.
7. Fu, X. G., Wang, J., Zeng, Y. H., Tan, F. W., He, J. L. Geochemistry and origin of rare earth elements (REEs) in the Shengli River oil shale, northern Tibet, China. *Chem. Erde-Geochem*., 2011, **71**(1), 21–30.
8. Xu, Z. Y. Tertiary system and its petroleum potential in the Lunpola Basin, Xizang (Tibet). *USGS Open File Rep*. 84–420, 1984, 6 pp.

9. Rowley, D. B., Currie, B. S. Palaeo-altimetry of the late Eocene to Miocene Lunpola basin, central Tibet. *Nature*, 2006, **439**(7077), 677–681.
10. Zhai, G. M. et al. (eds). Oil and gas fields in Qinghai and Xizang. In *Petroleum Geology of China*, Vol. 14. Petroleum Industry Press, Beijing, 1990 (in Chinese).
11. Du, B. W, Tan, F. W., Chen, M. Sedimentary features and petroleum geology of the Lunpola Basin, Xizang. *Sedimentary Geology and Tethyan Geology*, 2004, **24**(4), 46–54 (in Chinese).
12. Ma, L. X., Zhang, E. H., Ju, J. C., Lei, Q. L., Zhou, J. J. Basic characteristics of Palaeogene deposition systems tract in the Lunpola Basin, Xizang (Tibet). *Earth Sci*., 1996, **21**, 174–178 (in Chinese with English abstract).
13. Xia, J. B. Cenozoic of Baingoin and its borders, Xizang (Tibet). *Contrib. Geol. Qinghai-Xizang (Tibet) Plateau*, 1983, **3**, 243-254 (in Chinese with English summary).
14. Xu, Z. Y. The Tertiary and its petroleum potential in the Lunpola Basin, Tibet. *Oil Gas Geol*., 1980, **1**, 153–158.
15. Xu, Z. Y., Zhao, J. P., Wu, Z. L. On the Tertiary continental basins and their petroleum potential in Qinghai-Xizang (Tibet) Plateau with Lunpola Basin as example. *Contrib. Geol. Qinghai-Xizang (Tibet) Plateau*, 1985, **17**, 391–399 (in Chinese with English summary).
16. Xia, B. D., Liu, S. K. Stratigraphy (Lithostratic) of Xizang Autonomous Region. China University of Geosciences Press, Wuhan, 1997 (in Chinese).
17. DeCelles, P. G., Kapp, P., Ding, L., Gehrels, G. E. Late Cretaceous to middle Tertiary basin evolution in the central Tibetan Plateau: Changing environments in response to tectonic partitioning, aridification, and regional elevation gain. *Bull. Geol. Soc. Am.*, 2007, **119**(5–6), 654–680.
18. Peters, K. E. Guidelines for evaluating petroleum source rock using programmed pyrolysis. *AAPG Bull*., 1986, **70**(3), 318–329.
19. Petersen, H. I., Tru, V., Nielsen, L. H., Duc, N. A., Nytoft, H. P. Source rock properties of lacustrine mudstones and coals (Oligocene Dong Ho Formation), onshore Song Hong Basin, northern Vietnam. *J. Petrol. Geol*., 2005, **28**(1), 19–38.
20. Guthrie, J. M., Pratt, L. M. Geochemical indicators of depositional environment and source-rock potential for the Upper Ordovician Maquoketa Group, Illinois Basin. *AAPG Bull*., 1994, **78**(5), 744–757.
21. Talbot, M. R. The origins of lacustrine oil source rocks: evidence from the lakes of tropical Africa. In: Fleet, A. J., Kelts, K., Talbot, M. R. (eds.). Lacustrine Petroleum Source Rocks. Geological Society London Special Publications, Oxford, 1988, **40**, 29–43.
22. Talbot, M. R., Livingstone, D. A. Hydrogen index and carbon isotopes of lacustrine organic matter as lake level indicators. *Palaeogeogr. Palaeocl.*, 1989, **70**(1–3), 121–137.
23. Boreham, C. J., Summons, R. E., Roksandic, Z., Dowling, L. M., Hutton, A. C. Chemical, molecular and isotopic differentiation of organic facies in the Tertiary lacustrine Duaringa oil shale deposit, Queensland, Australia. *Org. Geochem*., 1994, **21**(6–7), 685–712.
24. Schouten, S., Rijpstra, W. I. C., Kok, M., Hopmans, E. C., Summons, R. E., Volkman, J. K., Sinninghe Damste, J. S. Molecular organic tracers of biogeochemical processes in a saline meromictic lake (Ace Lake). *Geochim. Cosmochim. Acta*, 2001, **65**(10), 1629–1640.

25. Schidlowski, M., Gorzawski, H., Dor, I. Carbon isotopic variations in a solar pond microbial mat: role of environmental gradients as steering variables. *Geochim. Cosmochim. Acta*, 1994, **58**(10), 2289–2298.
26. Lewan, M. D. Stable carbon isotopes of amorphous kerogens from Phanerozoic sedimentary rocks. *Geochim. Cosmochim. Acta,* 1986, **50**(8), 1583–1591.
27. Taylor, P., Bennett, B., Jones, M., Larter, S. The effect of biodegradation and water washing on the occurrence of alkylphenols in crude oils. *Org. Geochem.*, 2001, **32**(2), 341–358.
28. Meyers, P. A. Organic geochemical proxies of paleoceanographic, paleolimnologic, and paleoclimatic processes. *Org. Geochem*., 1997, **27**(5–6), 213–250.
29. Tissot, B. P., Welte, D. H. *Petroleum Formation and Occurrence*. Springer-Verlag, Berlin, New York, 1984.
30. Kotarba, M. J., Clayton, J. L. A stable carbon isotope and biological marker study of Polish bituminous coals and carbonaceous shales. *Int. J. Coal Geol.*, 2003, **55**(2–4), 73–94.
31. Koopmans, M. P., Rijpstra, W. I. C., Klapwijk, M. M., Leeuw, J. W. de, Lewan, M. D., Sinninghe Damste, J. S. A thermal and chemical degradation approach to decipher pristane and phytane precursors in sedimentary organic matter. *Org. Geochem*., 1999, **30**(9), 1089–1104.
32. Peters, K. E., Walters, C. C., Moldowan, J. M. *The Biomarker Guide*. Cambridge, Cambridge University Press, 2005.
33. Haven, H. L. ten, Leeuw, J. W. de, Rullkötter, J., Sinninghe Damsté, J. S. Restricted utility of the pristane/phytane ratio as palaeoenvironmental indicator. *Nature*, 1987, **330**(6149), 641–643.
34. Wang, L. C., Wang, C. S., Li, Y. L., Zhu, L. D., Wei, Y. S. Sedimentary and organic geochemical investigation of tertiary lacustrine oil shale in the central Tibetan plateau: Palaeolimnological and palaeoclimatic significances. *Int. J. Coal Geol.,* 2011, **86**(2–3), 254–265.
35. Dai, S., Ren, D., Tang, Y., Shao, L., Li, S. Distribution, isotopic variation and origin of sulfur in coals in the Wuda coalfield, Inner Mongolia, China. *Int. J. Coal Geol*., 2002, **51**(4), 237–250.
36. Jiang, Z. S., Fowler, M. G. Carotenoid-derived alkanes in oils from northwestern China. *Org. Geochem*., 1986, **10**(4–6), 831–839.
37. Carroll, A. R., Brassell, S. C., Graham, S. A. Upper Permian lacustrine oil shales, southern Junggar basin, northwest China. *AAPG Bull.*, 1992, **76**(12), 1874–1902.
38. Brassell, S. C., Sheng, G. Y., Fu, J. M., Eglinton, G. Biological markers in lacustrine Chinese oil shales. In: Fleet, A. J., Kelts, K., Talbot, M. R. (eds.). *Lacustrine Petroleum Source Rocks*. Geological Society Special Publication, Oxford, 1988, **40**, 299–308.
39. Fu, J. M., Sheng, G. Y., Peng, P. G., Brassell, S. C., Eglinton, G., Jiang, J. G. Peculiarities of salt lake sediments as potential source rocks in China. *Org. Geochem.*, 1986, **10**(1–3), 119–126.
40. Moldowan, J M., Seifert, W. K., Gallegos, E. J. Relationship between petroleum composition and depositional environment of petroleum source rocks. *AAPG Bull*., 1985, **69**(8), 1255–1268.
41. Sinninghe Damste, J. S., Kenig, F., Koopmans, M. P., Köster, J., Schouten, S., Hayes, J. M., Leeuw, J. W. de. Evidence for gammacerane as an indicator of water column stratification. *Geochim. Cosmochim. Acta*, 1995, **59**(9), 1895–1900.

42. Peters, K. E., Moldowan, J. M. *The Biomarker Guide: Interpreting Molecular Fossils in Petroleum and Ancient Sediments*. Englewood Cliffs, NJ, Prentice Hall, 1993.
43. Huang, W.-Y, Meinschein, W G. Sterols as ecological indicators. *Geochim. Cosmochim. Acta*, 1979, **43**(5), 739–745.
44. Czochanska, Z., Gilbert, T. D., Philp, R. P., Sheppard, C. M., Weston, R. J., Wood, T. A., Woolhouse, A. D. Geochemical application of sterane and triterpane biomarkers to a description of oils from the Taranaki Basin in New Zealand. *Org. Geochem.*, 1988, **12**(2), 123–135.
45. Volkman, J. K. A review of sterol markers for marine and terrigenous organic matter. *Org. Geochem.*, 1986, **9**(2), 83–99.
46. Dupont-Nivet, G., Krijgsman, W., Langereis, C. G., Abels, H. A., Dai, S., Fang, X. M. Tibetan plateau aridification linked to global cooling at the Eocene–Oligocene transition. *Nature*, 2007, **445**(7128), 635–638.
47. Dupont-Nivet, G., Hoorn, C., Konert, M. Tibetan uplift prior to the Eocene-Oligocene climate transition: evidence from pollen analysis of the Xining Basin. *Geology*, 2008, **36**(12), 987–990.
48. Harris, N. The elevation history of the Tibetan Plateau and its implications for the Asian monsoon. *Palaeogeogr. Palaeocl.*, 2006, **241**(1), 4–15.
49. Raymo, M. E., Ruddiman, W. F. Tectonic forcing of late Cenozoic climate. *Nature*, 1992, **359**(6391), 117–122.

Presented by J. Boak
Received August 2, 2012